Nonlinear State Estimation by Adaptive Embedded RBF Modules

Chengyu Gan
Graduate Research Assistant

Kourosh Danai
Professor

Department of Mechanical and Industrial Engineering,
University of Massachusetts,
Amherst, MA 01003-2210

A modeling compensation method is introduced to enhance the performance of the extended Kalman filter (EKF) in coping with the uncertainty of estimation model. In this method, single-input single-output radial basis function (RBF) modules are embedded within the nonlinear estimation model to provide additional degrees of freedom for model adaptation. The weights of the embedded RBF modules are adapted by the EKF, concurrent with state estimation. This compensation method is tested in application to a benchmark problem. Simulation results indicate that the RBF modules provide the means to model the uncertain components of the estimation model within their range of variation.
[DOI: 10.1115/1.1341198]

1 Introduction

State estimation is an integral part of modular adaptive control [1], and is important for model-based fault detection and diagnosis [2]. For linear observable time-invariant plants, a Luenberger Observer or Kalman Filter [3,4] can be used to estimate the states, but these observers have limited applicability to nonlinear plants [5–9]. The predominant obstacle to estimation of nonlinear plants' states is the added dependence of their observability on inputs [10], which precludes assurance of uniform observability, except for specific cases and under stringent conditions [11].

Among nonlinear observers [12], the Extended Kalman Filter (EKF) is used extensively because of its generality and recursive configuration [13]. For deterministic nonlinear time-invariant plants with bounded error covariances, the EKF is shown to function as a quasi-local observer [14]. It is also shown that boundedness of error covariances requires observability to be satisfied for the linearized model along the estimation trajectory. Another nonlinear observer is the sliding mode observer, which is basically a modified Luenberger observer with additional switching terms to guarantee robustness against modeling errors and uncertainties [15,16]. The sliding mode observer, however, is only applicable to plants with specific structures [15,17,18]. Nonlinear observers have also been developed that rely on transforming the nonlinear model to observer canonical form [6,19], but these observers are only applicable when such transformation is possible.

In order to provide state estimation of nonlinear plants in presence of modeling uncertainty and/or time-variability, adaptive observers have been developed to update the model on-line in response to the measured outputs [20]. The underlying model of these observers is generally linear with respect to parameters, therefore, for application to nonlinear plants the model needs to be linearly parametrizable [1]. The most noted effort in this category is the adaptive observer introduced by Kreisselmeier [21] which performs parameter and state estimation separately. This observer was later adopted in the form of a Hopfield network by Shoureshi and Chu [22], where the parameters and states of the linear model were estimated by minimizing a Lyapunov function defined in terms of the weights of the Hopfield network. Although it is shown that adaptive observers can guarantee boundedness of parameter and state estimates, those guarantees are generally made for exact models with unknown parameters. No nonlinear observer has been developed to date that can effectively cope with structural uncertainty and/or time-variability.

In order to avoid linear parametrization of nonlinear models, neural network-based adaptive observers have been developed [8,9]. One such observer uses a feedforward neural network to approximate the nonlinear part of a single-input single-output plant within a Luenberger-type observer [9]. Another observer uses a fuzzy neural network that is parameterized to provide first derivatives of the state and output functions of the plant model [8], as required by EKF. This neural network is trained off-line by supervised learning, before it is used as the estimation model by EKF. In both scenarios, the neural network has a 'black box' format, and requires extensive training before it can be used for estimation.

The purpose of this paper is to introduce a compensation method to cope with the uncertainty of the estimation model. In this method, instead of estimating the uncertain parameters of the estimation model directly, the parameters are modeled by adaptable single-input single-output Radial Basis Function (RBF) modules that are embedded within the estimation model. The weights of the RBF modules are initially set to zero so as to assure the same dynamics as the estimation model, but are subsequently trained by EKF in tandem with state estimation to yield an adaptive observer. This observer is generic and is shown to compensate for time-variability when tested in a benchmark problem.

2 Embedding RBF Modules

The purpose of embedding RBF modules into the estimation model is to provide additional degrees of freedom for adaptation. Let the exact model of the plant be represented by the state-space model:

$$\mathbf{x}(k+1)=\mathbf{\Phi}[\mathbf{x}(k),\mathbf{u}(k)]+\mathbf{w} \tag{1}$$

$$\mathbf{y}(k)=\mathbf{\Psi}[\mathbf{x}(k),\mathbf{u}(k)]+\mathbf{v} \tag{2}$$

where $\mathbf{x}(k)\in R^n$, $\mathbf{u}(k)\in R^p$, and $y(k)\in R^m$ represent the states, inputs, and outputs, respectively, $\mathbf{w}$ and $\mathbf{v}$ denote uncorrelated Gaussian noise, and $\mathbf{\Phi}$ and $\mathbf{\Psi}$ represent nonlinear state and output functions, respectively. It is often the case that one can decompose the state equations into single-input single-output (SISO) subfunctions, even though one may not know the exact form of these sub-functions. This two-level view of the plant model is expressed by rewriting the state equations as:

$$\mathbf{x}(k+1)=\mathbf{F}^*[f_1^{s*}(\xi),f_2^{s*}(\xi),\ldots]|_k+\mathbf{w} \tag{3}$$

$$\mathbf{y}(k)=\mathbf{G}^*[f_1^{o*}(\xi),f_2^{o*}(\xi),\ldots]|_k+\mathbf{v} \tag{4}$$

where $\mathbf{F}^*$ and $\mathbf{G}^*$ define the known relationship between the subfunctions f_i, and ξ represents a dummy variable of either x_i or

Contributed by the Dynamic Systems and Control Division for publication in the JOURNAL OF DYNAMIC SYSTEMS, MEASUREMENT, AND CONTROL. Manuscript received by the Dynamic Systems and Control Division October 5, 1999. Associate Editor: S. Fassois.

u_j. In the above representation, the time step k in time-dependent variables is omitted for brevity, superscript * signifies exactness, superscripts s and o denote association with a state or output equation, respectively, and the sub-functions $f^{s*}s$ and $f^{o*}s$ represent SISO sub-functions of x_i or u_j. For instance, the state equation

$$x(k+1)=\frac{\sin(x(k))\cos(u(k))+u(k)^2}{1+x(k)^2} \tag{5}$$

can be defined by four sub-functions:

$$f_1^{s*}(x)=\sin(x),\quad f_2^{s*}(x)=x^2,\quad f_3^{s*}(u)=\cos(u),\quad f_4^{s*}(u)=u^2 \tag{6}$$

to represent the state equation $x(k+1)$ as

$$x(k+1)=\frac{f_1^{s*}(x)f_3^{s*}(u)+f_4^{s*}(u)}{1+f_2^{s*}(x)}\Big|_k$$
$$=F^*(f_1^{s*}(x),f_2^{s*}(x),f_3^{s*}(u),f_4^{s*}(u))|_k \tag{7}$$

For the transformation of the plant model into Eqs. (3) and (4), the overall relationship between the sub-functions f^* (i.e., $\mathbf{F}^*$ and $\mathbf{G}^*$) needs to be known, but the exact form of the individual SISO sub-functions (i.e., f^*) is not required. To compensate for the inaccuracy of individual sub-functions in the estimation model of the plant, RBF modules are added to each approximated SISO sub-function. In the proposed method, each RBF has the input-output relationship

$$o_l(\xi_j)=e^{(-|\xi_j-c_l|^2/\sigma^2)} \tag{8}$$

where c_l and σ denote the center and standard deviation of the RBF, respectively. By lining up a series of these RBFs along the ξ_j axis, an RBF module is formed having the output

$$O_i(\xi_j)=\sum_{l=1}^{N_i}\theta_l e^{(-|\xi_j-c_l|^2/\sigma^2)}=\sum_{l=1}^{N_i}\theta_l\Omega(\xi_j,c_l) \tag{9}$$

The number of RBFs per each module can be determined according to the precision required of each module [23], with the centers of individual RBFs positioned evenly along the ξ_j axis. The addition of these modules to individual sub-functions of the estimation model then yields

$$f_i^\theta(\xi,\theta)=f_i(\xi)+f_i^\theta(\xi)=f_i(\xi)+\sum_{l=1}^{N_i}\theta_l\Omega(\xi,c_l) \tag{10}$$

According to the above convention, each modified sub-function in the transformed model is composed of two components: an analytical component, $f_i(\xi)$, which provides an approximation of its counterpart in the exact model, and an embedded RBF module, $f_i^\theta(\xi)$, to compensate for the discrepancy between the approximate sub-function and its exact counterpart (see Fig. 1). The embedding process is demonstrated for our example problem. Let us assume that the estimation model of the plant in Eq. (5) is defined as

$$\hat{x}(k+1)=\frac{\cos(\hat{x}(k))\sin(u(k))+u(k)}{1+\hat{x}(k)^3}$$

where $f_1^s(\hat{x})=\cos(\hat{x})$, $f_2^s(\hat{x})=\hat{x}^3$, $f_3^s(u)=\sin(u)$, and $f_4^s(u)=u$ are approximations of their counterparts f_i^{s*}. Then embedding the RBF modules into this estimation model will yield the RBF-embedded model,

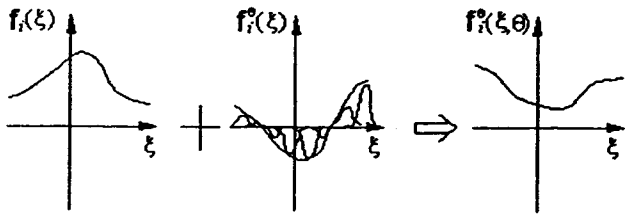

Fig. 1 Illustration of the modified sub-function when embedded by an RBF network

$$\hat{x}(k+1)=F^*(f_1^{s\theta}(\hat{x},\theta_1),f_2^{s\theta}(\hat{x},\theta_2),f_3^{s\theta}(u,\theta_3),f_4^{s\theta}(u,\theta_4))|_k$$
$$=\frac{f_1^{s\theta}(\hat{x},\theta_1)f_3^{s\theta}(u,\theta_3)+f_4^{s\theta}(u,\theta_4)}{1+f_2^{s\theta}(\hat{x},\theta_2)}\Big|_k$$
$$=\frac{\{\cos(\hat{x})+f_1^\theta(\hat{x})\}\{\sin(u)+f_3^\theta(u)\}+\{u+f_4^\theta(u)\}}{1+\{\hat{x}^3+f_2^\theta(\hat{x})\}}\Big|_k$$

As illustrated graphically in Fig. 1, the spatial nature of the RBF modules suggests a unique set of weights $\boldsymbol{\theta}^*$ for them so long as $\sigma/h\leq 1/\sqrt{\ln 3}$ (for proof see [23]).

Following the above strategy, the RBF-embedded model that approximates Eqs. (3) and (4) will have the form:

$$\hat{\mathbf{x}}(k+1)=\mathbf{F}^*[f_i^{s\theta}(\xi,\boldsymbol{\theta}_i^s),\ldots]|_k+\hat{\mathbf{w}} \tag{11}$$

$$\hat{\mathbf{y}}(k)=\mathbf{G}^*[f_j^{o\theta}(\xi,\boldsymbol{\theta}_j^o),\ldots]|_k+\hat{\mathbf{v}} \tag{12}$$

where the $f_i^{s\theta}(\xi,\boldsymbol{\theta}_i^s)$ and $f_j^{o\theta}(\xi,\boldsymbol{\theta}_j^o)$ denote embedded counterparts of sub-functions $f_i^{s*}(\xi)$ and $f_j^{o*}(\xi)$, respectively. The adaptation of the RBF-embedded model is performed by adjusting the weights of the radial basis functions. Initially, the weights of RBF modules are set to zero, so that they can be adapted during a training session in response to the measured plant outputs. Training of the RBF weight vector $\hat{\boldsymbol{\theta}}$, that includes the weights of all of the RBF modules, will be performed by EKF, in tandem with estimation of the plant states. The EKF algorithm, as applied to the RBF-embedded model, has the form

$$\hat{\mathbf{z}}(k+1)=\mathbf{f}_e(\hat{\mathbf{x}}(k),\mathbf{u}(k),\hat{\boldsymbol{\theta}})+\mathbf{G}(k)[\mathbf{y}(k)-\mathbf{G}^*(\hat{\mathbf{x}}(k),\mathbf{u}(k),\hat{\boldsymbol{\theta}})] \tag{13}$$

$$\mathbf{G}(k)=\mathbf{F}(k)\mathbf{P}(k)\mathbf{H}^T(k)\times[\mathbf{H}(k)\mathbf{P}(k)\mathbf{H}^T(k)+\hat{\mathbf{Q}}_e^v]^{-1} \tag{14}$$

$$\mathbf{P}(k+1)=\mathbf{F}(k)\mathbf{P}(k)\mathbf{F}^T(k)+\hat{\mathbf{Q}}_e^w$$
$$-\mathbf{G}(k)[\mathbf{H}(k)\mathbf{P}(k)\mathbf{H}^T(k)+\hat{\mathbf{Q}}_e^v]\mathbf{G}(k) \tag{15}$$

where

$$\hat{\mathbf{z}}(k)=[\hat{\mathbf{x}}(k)\ \hat{\boldsymbol{\theta}}]^T,\quad \mathbf{f}_e(\hat{\mathbf{x}}(k),\mathbf{u}(k),\hat{\boldsymbol{\theta}})=\begin{bmatrix}\mathbf{F}^*(\hat{\mathbf{x}}(k),\mathbf{u}(k),\hat{\boldsymbol{\theta}})\\ \hat{\boldsymbol{\theta}}\end{bmatrix}$$

$$\mathbf{F}(k)=\frac{\partial\mathbf{f}_e(\hat{\mathbf{x}}(k),\mathbf{u}(k),\hat{\boldsymbol{\theta}})}{\partial\mathbf{z}}\Big|_{\mathbf{z}=\hat{\mathbf{z}}(k)}=\begin{bmatrix}\mathbf{A}(k) & \mathbf{M}(k)\\ \mathbf{0} & \mathbf{I}\end{bmatrix}$$

$$\mathbf{H}(k)=\frac{\partial\mathbf{G}^*(\hat{\mathbf{x}}(k),\mathbf{u}(k),\hat{\boldsymbol{\theta}})}{\partial\mathbf{z}}\Big|_{\mathbf{z}=\hat{\mathbf{z}}(k)}=[\mathbf{C}(k)\ \ \mathbf{D}(k)]$$

$$\hat{\mathbf{Q}}^w=E\{\mathbf{w}^T\mathbf{w}\},\quad \hat{\mathbf{Q}}^v=E\{\mathbf{v}^T\mathbf{v}\}$$

$$\hat{\mathbf{Q}}_e^w=\begin{bmatrix}\hat{\mathbf{Q}}^w & \mathbf{0}\\ \mathbf{0} & \mathbf{0}\end{bmatrix},\quad \hat{\mathbf{Q}}_e^v=\begin{bmatrix}\hat{\mathbf{Q}}^v\\ \mathbf{0}\end{bmatrix}$$

and

$$\mathbf{A}(k)=\left.\frac{\partial \mathbf{F}^*(\hat{\mathbf{x}}(k),\mathbf{u}(k),\hat{\boldsymbol{\theta}})}{\partial \mathbf{x}}\right|_{\mathbf{z}=\hat{\mathbf{z}}(k)}$$

$$\mathbf{M}(k)=\left.\frac{\partial \mathbf{F}^*(\hat{\mathbf{x}}(k),\mathbf{u}(k),\hat{\boldsymbol{\theta}})}{\partial \boldsymbol{\theta}}\right|_{\mathbf{z}=\hat{\mathbf{z}}(k)}$$

$$\mathbf{C}(k)=\left.\frac{\partial \mathbf{G}^*(\hat{\mathbf{x}}(k),\mathbf{u}(k),\hat{\boldsymbol{\theta}})}{\partial \mathbf{x}}\right|_{\mathbf{z}=\hat{\mathbf{z}}(k)}$$

$$\mathbf{D}(k)=\left.\frac{\partial \mathbf{G}^*(\hat{\mathbf{x}}(k),\mathbf{u}(k),\hat{\boldsymbol{\theta}})}{\partial \boldsymbol{\theta}}\right|_{\mathbf{z}=\hat{\mathbf{z}}(k)}$$

3 Convergence Issues

The extended Kalman Filter (EKF) is an approximate filter for nonlinear plants based on first-order linearization. For the nonlinear plant defined in Eqs. (1) and (2), it has been shown, using Lyapunov theory, that the convergence of EKF is guaranteed when either a good initial guess of the parameters is available or the plant satisfies weak nonlinearity condition in the sense that $\|\partial^2\Phi_{(\mathbf{x})}/\partial\mathbf{x}^2\|$ and $\|\partial^2\Psi_{(\mathbf{x})}/\partial\mathbf{x}^2\|$ is sufficiently small [14]. It is further shown that in order to ensure boundedness of the error covariances in EKF, an observability condition needs to be satisfied by the linearized model along the estimation trajectory. (Similar precondition for observability to ensure EKF convergence is derived by Ljung [24].)

Although the above convergence analysis provides general assurances about the performance of EKF, it cannot be directly extended to the proposed method since it does not consider the presence of modeling inaccuracy. To account for modeling inaccuracy, the analysis performed by Ljung [25] is adopted, which uses associated differential equations of the EKF:

$$\frac{d\boldsymbol{\theta}(t)}{dt}=\mathbf{R}(t)^{-1}\boldsymbol{\Omega}(\boldsymbol{\theta}(t)) \tag{16}$$

$$\frac{d\mathbf{R}(t)}{dt}=\boldsymbol{\Gamma}(\boldsymbol{\theta}(t))+\delta\mathbf{I}-\mathbf{R}(t) \tag{17}$$

where

$$\boldsymbol{\Omega}(\boldsymbol{\theta})=E\{\boldsymbol{\beta}(k)\mathbf{S}^{-1}(k)\boldsymbol{\varepsilon}(k)\}$$

$$\boldsymbol{\Gamma}(\boldsymbol{\theta})=E\{\boldsymbol{\beta}(k)\mathbf{S}^{-1}(k)\boldsymbol{\beta}(k)\}$$

and

$$\boldsymbol{\alpha}(k+1)=[\mathbf{A}(k)-\mathbf{K}(k)\mathbf{C}(k)]\boldsymbol{\alpha}(k)+[\mathbf{M}(k)-\mathbf{K}(k)\mathbf{D}(k)]$$

$$\boldsymbol{\beta}(k)=[\mathbf{C}(k)\boldsymbol{\alpha}(k)+\mathbf{D}(k)]^T$$

$$\mathbf{S}(k)=[\mathbf{H}(k)\mathbf{P}(k)\mathbf{H}^T(k)+\hat{\mathbf{Q}}_e^v]$$

$$\mathbf{G}(k)=[\mathbf{K}(k)\ \ \mathbf{L}(k)]$$

$$\boldsymbol{\varepsilon}(k)=\mathbf{y}(k)-\mathbf{G}^*(\hat{\mathbf{x}}(k),\mathbf{u}(k),\boldsymbol{\theta})$$

According to Ljung [24], if $D_s=\{\theta|(\mathbf{A}(\boldsymbol{\theta}),\hat{\mathbf{Q}}^w)$ is stabilizable and $(\mathbf{A}(\boldsymbol{\theta}), \mathbf{C}(\boldsymbol{\theta}))$ is observable$\}$, if the differential equations (16) and (17) have an invariant set D_c with domain of attraction $\boldsymbol{\theta}\in D_A$ which is a subset of D_s, if $\hat{\boldsymbol{\theta}}(k)$ belongs to a compact subset of D_A, and if $\hat{\mathbf{x}}(k)$ is bounded, then $\hat{\boldsymbol{\theta}}\rightarrow D_c$ with probability 1 as $k\rightarrow\infty$. The condition that requires $\hat{\boldsymbol{\theta}}(k)$ to belong to the compact subset D_A is usually enforced by various projection strategies [24]. The above theorem indicates that under the stated conditions the estimated parameter set $\boldsymbol{\theta}$ converges to an invariant set D_c. Now, in order to guarantee convergence of $\hat{\boldsymbol{\theta}}$ to $\boldsymbol{\theta}^*$, one needs to ensure that $\boldsymbol{\theta}^*\in D_c$, or that $\boldsymbol{\theta}^*$ belongs to a stationary point of Eq. (16) (i.e., $\boldsymbol{\Omega}(\boldsymbol{\theta}^*)=0$). It has been shown in [24] that $\boldsymbol{\Omega}(\boldsymbol{\theta}^*)=0$ when the error sequence $\{\boldsymbol{\varepsilon}(k,\boldsymbol{\theta}^*)\}$ is uncorrelated, which requires that the noise structure ($\hat{\mathbf{Q}}^w$ and $\hat{\mathbf{Q}}^v$) of the RBF-embedded model matches the actual one ($\mathbf{Q}^w$ and $\mathbf{Q}^v$) [24]. While an exact knowledge of the noise structure guarantees that the optimal set $\boldsymbol{\theta}^*$ belongs to the invariant set D_c, it does not necessarily ensure $\hat{\boldsymbol{\theta}}\rightarrow\boldsymbol{\theta}^*$, unless the initial guess $\hat{\boldsymbol{\theta}}(0)$ is selected relatively close to $\boldsymbol{\theta}^*$.

The conditions stated above only provide general guidelines about the convergence of the resulting adaptive observer. They indicate that the convergence of the EKF depends strongly on the initial guess $\hat{\boldsymbol{\theta}}(0)$, therefore, in cases where multiple stationary points exist and the optimal parameter $\boldsymbol{\theta}^*$ is one of them, only when the initial parameter $\hat{\boldsymbol{\theta}}(0)$ is set "close" to $\boldsymbol{\theta}^*$, $\hat{\boldsymbol{\theta}}$ would converge to $\boldsymbol{\theta}^*$ and would lead to $\hat{\mathbf{x}}\rightarrow\mathbf{x}$.

In order to strengthen the above convergence conditions, the EKF can be made to behave as a gradient descent algorithm. It has been shown by Ljung [24] that the EKF can be formatted to minimize the cost function $V(\hat{\boldsymbol{\theta}})=E\{\boldsymbol{\varepsilon}(k),\hat{\boldsymbol{\theta}})\}^2$, by changing the matrix $\mathbf{M}$ in the EKF algorithm to

$$\mathbf{M}(k)=\left.\frac{\partial \mathbf{F}^*(\hat{\mathbf{x}}(k),\mathbf{u}(k),\hat{\boldsymbol{\theta}})}{\partial \boldsymbol{\theta}}\right|_{\mathbf{z}=\hat{\mathbf{z}}(k)}+\left.\frac{\partial \mathbf{K}(\hat{\boldsymbol{\theta}})}{\partial \boldsymbol{\theta}}\boldsymbol{\varepsilon}(k)\right|_{\mathbf{z}=\hat{\mathbf{z}}(k)}$$

The computation of the matrix $\mathbf{M}$ in its new form will be facilitated greatly by parameterizing the matrix $\mathbf{K}$ in terms of $\boldsymbol{\theta}$, so that the second part of the relationship will have a closed form. Note that such a parameterization will result in a stronger resemblance of the learning algorithm to the general form of other adaptive observers:

$$\hat{\mathbf{x}}(k+1)=\mathbf{F}(\hat{\mathbf{x}}(k),\mathbf{u}(k),\hat{\boldsymbol{\theta}})+\mathbf{K}(\hat{\boldsymbol{\theta}})\boldsymbol{\varepsilon}(k)$$

$$\hat{\boldsymbol{\theta}}(k+1)=\mathbf{P}(\boldsymbol{\varepsilon}(k),\mathbf{u}(k),\hat{\boldsymbol{\theta}}(k))$$

which also have their gain matrix $\mathbf{K}$ parameterized in terms of $\boldsymbol{\theta}$ [1].

4 Evaluation

The effectiveness of the proposed adaptive observer is demonstrated in application to an induction motor benchmark problem [26]. This benchmark problem, which represents a multi-input multi-output plant, tests the performance of the proposed compensation method in coping with time-variability of the plant. The benchmark problem consists of a fifth order nonlinear model with two inputs. Only three state variables of the plant can be measured, so two of the states need to be estimated. The dynamical (stator-fixed frame) model in state-space form is defined as:

$$\mathbf{x}(k+1)=\mathbf{f}(\mathbf{x}(k))+\mathbf{g}_1u_1(u)+\mathbf{g}_2u_2(u) \tag{18}$$

where

$$\mathbf{f}(\mathbf{x})=\begin{bmatrix}\frac{n_pL_{sr}}{D_mL_r}(x_2x_5-x_3x_4)-\frac{R_m}{D_m}x_1-\frac{1}{D_m}\tau_L\\ -\frac{1}{T_r}x_2-n_px_1x_3+\frac{1}{T_r}L_{sr}x_4\\ n_px_1x_2-\frac{1}{T_r}x_3+\frac{1}{T_r}L_{sr}x_5\\ \frac{1}{T_r}\frac{L_{sr}}{\sigma L_sL_r}x_2+n_p\frac{L_{sr}}{\sigma L_sL_r}x_1x_3-\gamma x_4\\ -n_p\frac{L_{sr}}{\sigma L_sL_r}x_1x_2+\frac{1}{T_r}\frac{L_{sr}}{\sigma L_sL_r}x_3-\gamma x_5\end{bmatrix},$$

$$\mathbf{g}_1=\begin{bmatrix}0\\0\\0\\\frac{1}{\sigma L_s}\\0\end{bmatrix},\quad \mathbf{g}_2=\begin{bmatrix}0\\0\\0\\0\\\frac{1}{\sigma L_s}\end{bmatrix} \tag{19}$$

and the outputs are:

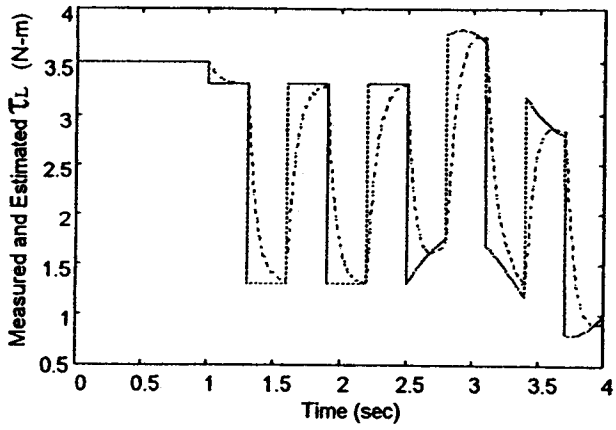

Fig. 2 Estimated values (dotted line) of the load torque τ_L by EKF using the nominal model

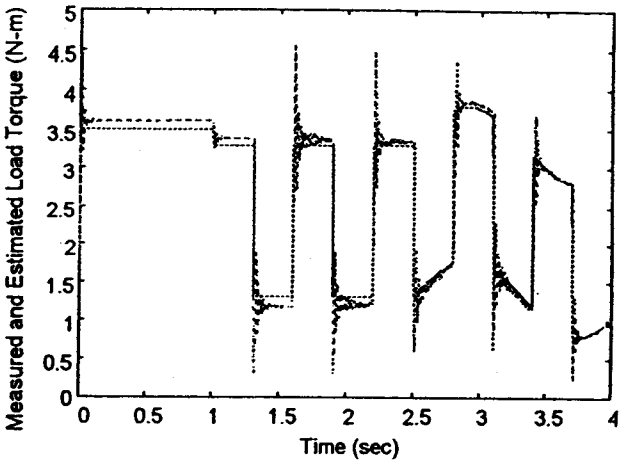

Fig. 3 Estimated values of the load torque by EKF using the RBF-embedded model

$$\mathbf{y}=\begin{bmatrix} x_1 \\ x_4 \\ x_5 \end{bmatrix}$$

In the above equations, the state vector $\mathbf{x}=[\omega\ \lambda_a\ \lambda_b\ i_a\ i_b]^T$ represents the rotor speed, ω, the rotor fluxes, λ_a and λ_b, and stator currents, i_a and i_b. The inputs u_1 and u_2 denote stator voltages and τ_L represents the load torque. The model parameters L_s, L_r, and L_{sr} denote the stator, rotor, and mutual inductance, respectively; σ, R_s, and R_r represent the total leakage factor, stator resistance, and rotor resistance, respectively; and D_m, R_m, and n_p denote the moment of inertia of the rotor, the mechanical viscous damping constant, and the number of pole pairs, respectively.

A natural occurrence with induction motors is a changing load torque, τ_L. As such, there is a need to estimate τ_L on-line. First, the performance of the EKF in estimating the parameter τ_L, having the approximate profile of a square wave, was tested. The estimated values of τ_L by the EKF are shown in Fig. 2. The results indicate that although the EKF provides a reasonably good estimate of the load torque τ_L at steady-state instances, it does not adequately represent its transients. In fact, the estimates provided by the EKF resemble a Fourier Series approximation of a square wave when it contains an inadequate number of harmonic components. This implies that the estimation model is underparametrized for representing such a fast-changing parameter.

The embedded RBF modules are to provide the extra degrees of freedom required for estimation of parameters like τ_L. To provide the extra degrees of freedom, the load torque was treated as a sub-function and was embedded with an RBF module. As the result, τ_L in Eq. (19) was replaced with τ_L', defined as

$$\tau_L'=\hat{\tau}_L+\sum_{i=1}^{N}\theta_i e^{[(\hat{\tau}_L(k)-c_i)^2/\delta^2]} \tag{20}$$

For this example, the number of RBFs was selected as 63 (i.e., $N=63$), which is within the range of RBFs needed to represent a function [23]. The weights θ_i of these RBFs, initially set to zeros, were then estimated by EKF along with $\hat{\tau}_L$, λ_a and λ_b. The estimated values of τ_L' are shown in Fig. 3. The results indicate that the estimated τ_L' provides a more accurate estimation of load torque dynamics, and that it takes about 3.5 s (or about 1200 sample points at the sampling rate of 3 ms) for the RBF weights to converge. It should be noted that once the weights converge to their true values, they provide an accurate representation of the sub-function, independent of its dynamics, as verified by the close estimation of the load torque τ_L' even when it deviates from the square wave format.

In order to explain the adaptation capacity of the embedded RBF module, one should study the modification made to the estimation model, namely, the approximation of τ_L by τ_L' in Eq. (20). In this case, τ_L represents the sub-function $f_i^{s*}(\xi)$ in Eq. (3), with $\xi=\tau_L$. As such, the modified sub-function, τ_L', ($f_i^{\theta}(\xi,\boldsymbol{\theta})$ in Eq. (10)) needs to be equal to τ_L, i.e., $f_i^{\theta}(\hat{\xi},\boldsymbol{\theta})=\xi$. To verify this point, the trained function τ_L' is plotted in Fig. 4 versus the actual τ_L. The results indicate that the function $\tau_L'=f^{\theta}(\hat{\tau}_L,\boldsymbol{\theta})$ is indeed equal to τ_L, and that it provides a one-to-one mapping of the load torque regardless of its time-variations. The estimated states Rotor Flux1 and Rotor Flux2 are shown in Fig. 5, to indicate the accurate estimation of the states resulted from the close estimation of the load torque function.

As shown by the application to this benchmark problem, the proposed compensation method provides additional flexibility for estimation of individual parameters. However, the flexibility provided is at the cost of additional computation to estimate the RBF weights. Naturally, there is a limit to how many RBF modules can be embedded into the estimation model. In cases where a single, although repeated, parameter needs to be estimated, say, the rotor constant T_r in Eq. (19), only one RBF module would be sufficient, since it can be used everywhere the parameter appears. However, if several parameters need to be estimated using RBF modules, then the computation load would increase significantly.

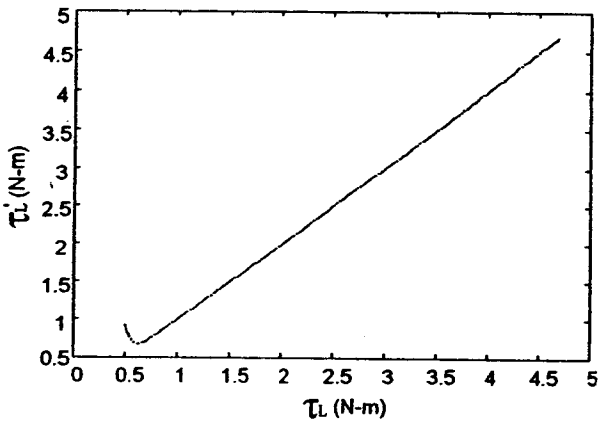

Fig. 4 The relationship between the modified sub-function τ_L' and τ_L as obtained by adapting the RBF weights

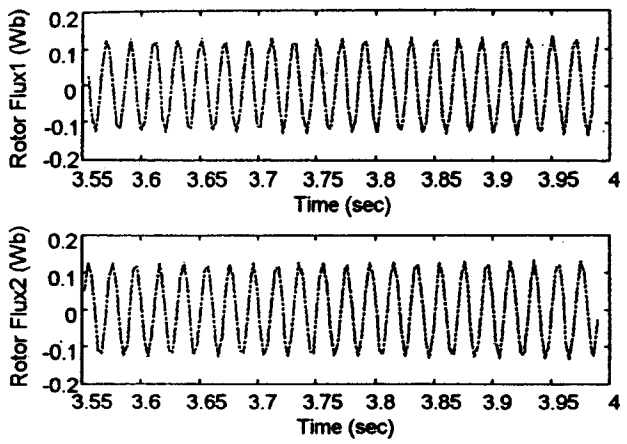

Fig. 5 Estimated values of the states Rotor Flux1 and Rotor Flux2 by EKF using the RBF-embedded model

5 Conclusion

A modeling compensation method is introduced that enhances the performance of the extended Kalman filter (EKF). This method embeds radial basis function (RBF) modules into the nonlinear estimation model so as to model its individual uncertain components. As such, this method provides an extra dimension to modeling where instead of estimating individual parameters online, as is currently done by EKF, they are modeled by RBF modules first and then computed in terms of the RBF weights. Convergence issues associated with the estimation of the RBF weights are discussed and the performance of the EKF using an RBF-embedded model is evaluated in application to a benchmark problem.

References

[1] Krstic, M., Kanellakopoulos, I., and Kokotovic, P., 1995, *Nonlinear and Adaptive Control Design*, Wiley, New York, NY.

[2] Frank, P. M., 1990, "Fault diagnosis in dynamic systems using analytical and knowledge-based redundancy-a survey and some new results," Automatica, **26**, No. 2, pp. 459–474.

[3] Gelb, A., 1974, *Applied Optimal Estimation*, MIT Press, Cambridge, MA.

[4] Luenberger, D. G., 1971, "An introduction to observers," IEEE Trans. Autom. Control, **AC16**, No. 6, pp. 596–602.

[5] Tse, E., and Athans, M., 1970, "Optimal minimal-order observer estimators for discrete linear time-varying systems," IEEE Trans. Autom. Control, **AC-15**, pp. 416–426.

[6] Bestle, D., and Zeitz, M., 1993, "Canonical form observer design for nonlinear time-variable systems," Int. J. Control, **38**, No. 2, pp. 419–431.

[7] Gauthier, J. P., and Kupka, I. A. K., 1994, "Observability and observer for nonlinear systems," SIAM J. Control Optim., **32**, No. 4, pp. 975–994.

[8] Chao, C. T., and Teng, C. C., 1996, "A fuzzy neural network based extended kalman filter," Int. J. Syst. Sci., **27**, No. 3, pp. 333–339.

[9] Kim, Y. H., Frank, L. L., and Chaouki, T. A., 1997, "A dynamic recurrent neural-network-based adaptive observer for a class of nonlinear systems," Automatica, **33**, No. 8, pp. 1539–1543.

[10] Gauthier, J. P., Hammouri, H., and Othman, S., 1992, "A simple observer for nonlinear systems: application to bioreactors," IEEE Trans. Autom. Control, **37**, pp. 875–880.

[11] Vidyasagar, M., 1993, *Nonlinear Systems Analysis*, Prentice-Hall, Englewood Cliffs, NJ.

[12] Misawa, E. A., and Hedrick, J. K., 1989, "Nonlinear observer-a state of the art survey," ASME J. Dyn. Syst., Meas., Control, **111**, pp. 344–352.

[13] Sorenson, H. W., 1985, *Kalman Filtering: Theory and Application*, IEEE Press, New York, N.Y.

[14] Song, Y., and Grizzle, J. W., 1992, "The extended kalman filter as a local asymptotic observer for nonlinear discrete-time systems," in *Proc. of the American Control Conference*, Chicago, IL, pp. 3365–3369.

[15] Drakunov, S., 1992, "Sliding mode observers based on equivalent control method," *Proc. of the 31st IEEE Conf. on Decision and Control*, Tucson, Arizona, pp. 2368–2369.

[16] Krishnaswami, V., and Rizzoni, G., 1995, "Vehicle steering system state estimation using sliding mode observers," *Proc. of the 34th Conference on Decision & Control*, New Orleans, LA, pp. 3391–3396.

[17] Drakunov, S. V., 1983, "An adaptive quasioptimal filter with discontinuous parameters," Autom. Remote Control, **44**, No. 2, pp. 76–86.

[18] Slotine, J. E., Hedrick, J. K., and Hedrick, M. E. A., 1987, "On sliding observers," ASME J. Dyn. Syst., Meas., Control, **109**, pp. 245–252.

[19] Krener, A. J., and Isidori, W., 1983, "Linearization by output injection and nonlinear observer," Syst. Control Lett., **3**, pp. 47–52.

[20] Narendra, K. S., and Annaswamy, A. M., 1989, *Stable Adaptive Systems* Prentice Hall, Englewood Cliffs, NJ.

[21] Kreisselmeier, G., 1977, "Adaptive observers with exponential rate of convergence," IEEE Trans. Autom. Control, **22**, pp. 2–8.

[22] Shoureshi, R., and Chu, R., 1993, "Hopfield-based adaptive observers: next generation of luenberger state estimators," *IEEE Int. Conference on Neural Networks*, Piscataway, New Jersey, Apr., pp. 1289–1294.

[23] Gan, C., 2000, "*Embedded radial basis function networks to compensate for modeling uncertainty of nonlinear dynamic systems*," Doctoral dissertation, University of Massachusetts Amherst, Department of Mechanical and Industrial Engineering.

[24] Ljung, L., 1979, "Asymptotic behavior of the extended kalman filter as a parameter estimator for linear systems," IEEE Trans. Autom. Control, **AC24**, No. 1, pp. 36–50.

[25] Ljung, L., 1977, "Analysis of recurive stochastic algorithms," IEEE Trans. Autom. Control, **AC22**, No. 4, pp. 551–575.

[26] Ortega, R., Chang, G., and Mendes, E., 1998, *Control of Induction Motors: A Benchmark Problem, for Nonlinear Control*. http://www.supelec.fr/invi/lss/fr/personels/ortega/benchmi/benchmi.html.